30. M. X. Kirby, B. MacFadden, *Palaeogeogr. Palaeoclimatol. Palaeoecol.* **228**, 193–202 (2005).

ACKNOWLEDGMENTS

Supported by Ecopetrol-ICP "Cronología de la Deformación en las Cuencas Subandinas," Smithsonian Institution, Uniandes P12. 160422.002/001, Autoridad del Canal de Panama (ACP), the Mark Tupper Fellowship, Ricardo Perez S.A.; NSF grant EAR 0824299 and OISE, EAR, DRL 0966884, Colciencias, and the National Geographic Society. We thank N. Hoyos, D. Villagomez, A. O'Dea, C. Bustamante, O. Montenegro, and C. Ojeda. All the data reported in this manuscript are presented in the main paper and in the supplementary materials.

SUPPLEMENTARY MATERIALS

www.sciencemag.org/content/348/6231/226/suppl/DC1
Materials and Methods
Supplementary Text
Figs. S1 to S3
Tables S1 to S5
References (*31*–*42*)

12 November 2014; accepted 2 March 2015
10.1126/science.aaa2815

EARTH HISTORY

Ocean acidification and the Permo-Triassic mass extinction

M. O. Clarkson,[1]*† S. A. Kasemann,[2] R. A. Wood,[1] T. M. Lenton,[3] S. J. Daines,[3] S. Richoz,[4] F. Ohnemueller,[2] A. Meixner,[2] S. W. Poulton,[5] E. T. Tipper[6]

Ocean acidification triggered by Siberian Trap volcanism was a possible kill mechanism for the Permo-Triassic Boundary mass extinction, but direct evidence for an acidification event is lacking. We present a high-resolution seawater pH record across this interval, using boron isotope data combined with a quantitative modeling approach. In the latest Permian, increased ocean alkalinity primed the Earth system with a low level of atmospheric CO_2 and a high ocean buffering capacity. The first phase of extinction was coincident with a slow injection of carbon into the atmosphere, and ocean pH remained stable. During the second extinction pulse, however, a rapid and large injection of carbon caused an abrupt acidification event that drove the preferential loss of heavily calcified marine biota.

The Permo-Triassic Boundary (PTB) mass extinction, at ~252 million years ago (Ma), represents the most catastrophic loss of biodiversity in geological history and played a major role in dictating the subsequent evolution of modern ecosystems (*1*). The PTB extinction event spanned ~60,000 years (*2*) and can be resolved into two distinct marine extinction pulses (*3*). The first occurred in the latest Permian [Extinction Pulse 1 (EP1)] and was followed by an interval of temporary recovery before the second pulse (EP2), which occurred in the earliest Triassic. The direct cause of the mass extinction is widely debated, with a diverse range of overlapping mechanisms proposed, including widespread water column anoxia (*4*), euxinia (*5*), global warming (*6*), and ocean acidification (*7*).

Models of PTB ocean acidification suggest that a massive and rapid release of CO_2 from Siberian Trap volcanism acidified the ocean (*7*). Indirect evidence for acidification comes from the interpretation of faunal turnover records (*3*, *8*), potential dissolution surfaces (*9*), and Ca isotope data (*7*). A rapid input of carbon is also potentially recorded in the negative carbon isotope excursion (CIE) that characterizes the PTB interval (*10*, *11*). The interpretation of these records is, however, debated (*12*–*16*) and is of great importance to understanding the current threat of anthropogenically driven ocean acidification (*11*).

To test the ocean acidification hypothesis, we have constructed a proxy record of ocean pH across the PTB using the boron isotope composition of marine carbonates ($\delta^{11}B$) (*17*). We then used a carbon cycle model (supplementary text) to explore ocean carbonate chemistry and pH scenarios that are consistent with our $\delta^{11}B$ data and published records of carbon cycle disturbance and environmental conditions. Through this combined geochemical, geological, and modeling approach, we are able to produce an envelope that encompasses the most realistic range in pH, which then allows us to resolve three distinct chronological phases of carbon cycle perturbation, each with very different environmental consequences for the Late Permian–Early Triassic Earth system.

We analyzed boron and carbon isotope data from two complementary transects in a shallow marine, open-water carbonate succession from the United Arab Emirates (U.A.E.), where depositional facies and stable carbon isotope ratio ($\delta^{13}C$) are well constrained (*18*). During the PTB interval, the U.A.E. formed an expansive carbonate platform that remained connected to the central Neo-Tethyan Ocean (Fig. 1A) (*18*). Conodont stratigraphy and the distinct $\delta^{13}C$ curve are used to constrain the age model (*17*).

The PTB in the Tethys is characterized by two negative $\delta^{13}C$ excursions interrupted by a short-term positive event (*10*). There is no consensus as to the cause of this "rebound" event and so we instead focus on the broader $\delta^{13}C$ trend. Our $\delta^{13}C$ transect (Fig. 1B) starts in the Changhsingian (Late Permian) with a gradual decreasing trend, interrupted by the first negative shift in $\delta^{13}C$ at EP1 (at 53 m, ~251.96 Ma) (Figs. 1B and 2). This is followed by the minor positive rebound event (at 54 m, ~251.95 Ma) (Figs. 1B and 2) before the minima of the second phase of the negative CIE (58 to 60 m, ~251.92 Ma) (Figs. 1B and 2) that marks the PTB itself. After the CIE minimum, $\delta^{13}C$ gradually increases to ~1.8 per mil (‰) and remains relatively stable during the earliest Triassic and across EP2.

Our boron isotope record shows a different pattern to the carbon isotope excursion. The boron isotope ratio ($\delta^{11}B$) is persistently low (Fig. 1C) at the start of our record during the late-Changhsingian, with an average of 10.9 ± 0.9‰ (1σ). This is in agreement with $\delta^{11}B$ values (average of 10.6 ± 0.6‰, 1σ) reported for early-Permian brachiopods (*19*). Further up the section (at ~40 m, ~252.04 Ma) (Fig. 1C), there is a stepped increase in $\delta^{11}B$ to 15.3 ± 0.8‰ (propagated uncertainty, 2σf) and by implication an increase in ocean pH of ~0.4 to 0.5 (Fig. 2). $\delta^{11}B$ values then remain relatively stable, scattering around 14.7 ± 1.0‰ (1σ) and implying variations within 0.1 to 0.2 pH, into the Early Griesbachian (Early Triassic) and hence across EP1 and the period of carbon cycle disturbance (Figs. 1 and 2).

After the $\delta^{13}C$ increase and stabilization (at ~85 m, ~251.88 Ma) (Fig. 1), $\delta^{11}B$ begins to decrease rapidly to 8.2 ± 1.2‰ (2σf), implying a sharp drop in pH of ~0.6 to 0.7. The $\delta^{11}B$ minimum is coincident with the interval identified as EP2. This ocean acidification event is short-lived (~10,000 years), and $\delta^{11}B$ values quickly recover toward the more alkaline values evident during EP1 (average of ~14‰).

The initial rise in ocean pH of ~0.4 to 0.5 units during the Late Permian (Fig. 2) suggests a large increase in carbonate alkalinity (*20*). We are able to simulate the observed rise in $\delta^{11}B$ and pH through different model combinations of increasing silicate weathering, increased pyrite deposition (*21*), an increase in carbonate weathering, and a decrease in shallow marine carbonate depositional area (supplementary text). Both silicate weathering and pyrite deposition result in a large drop in partial pressure of CO_2 (P_{CO_2}) (and temperature) for a given increase in pH and saturation state (Ω). There is no evidence for a large drop in P_{CO_2}, and independent proxy data

[1]School of Geosciences, University of Edinburgh, West Mains Road, Edinburgh EH9 3FE, UK. [2]Faculty of Geosciences and MARUM–Center for Marine Environmental Sciences, University of Bremen, 28334 Bremen, Germany. [3]College of Life and Environmental Sciences, University of Exeter, Laver Building, North Parks Road, Exeter EX4 4QE, UK. [4]Institute of Earth Sciences, NAWI Graz, University of Graz, Heinrichstraße 26, 8010 Graz, Austria. [5]School of Earth and Environment, University of Leeds, Leeds LS2 9JT, UK. [6]Department of Earth Sciences, University of Cambridge, Downing Street, Cambridge CB2 3EQ, UK.
*Corresponding author. E-mail: matthew.clarkson@otago.ac.nz
†Present address: Department of Chemistry, University of Otago, Union Street, Dunedin, 9016, Post Office Box 56, New Zealand.

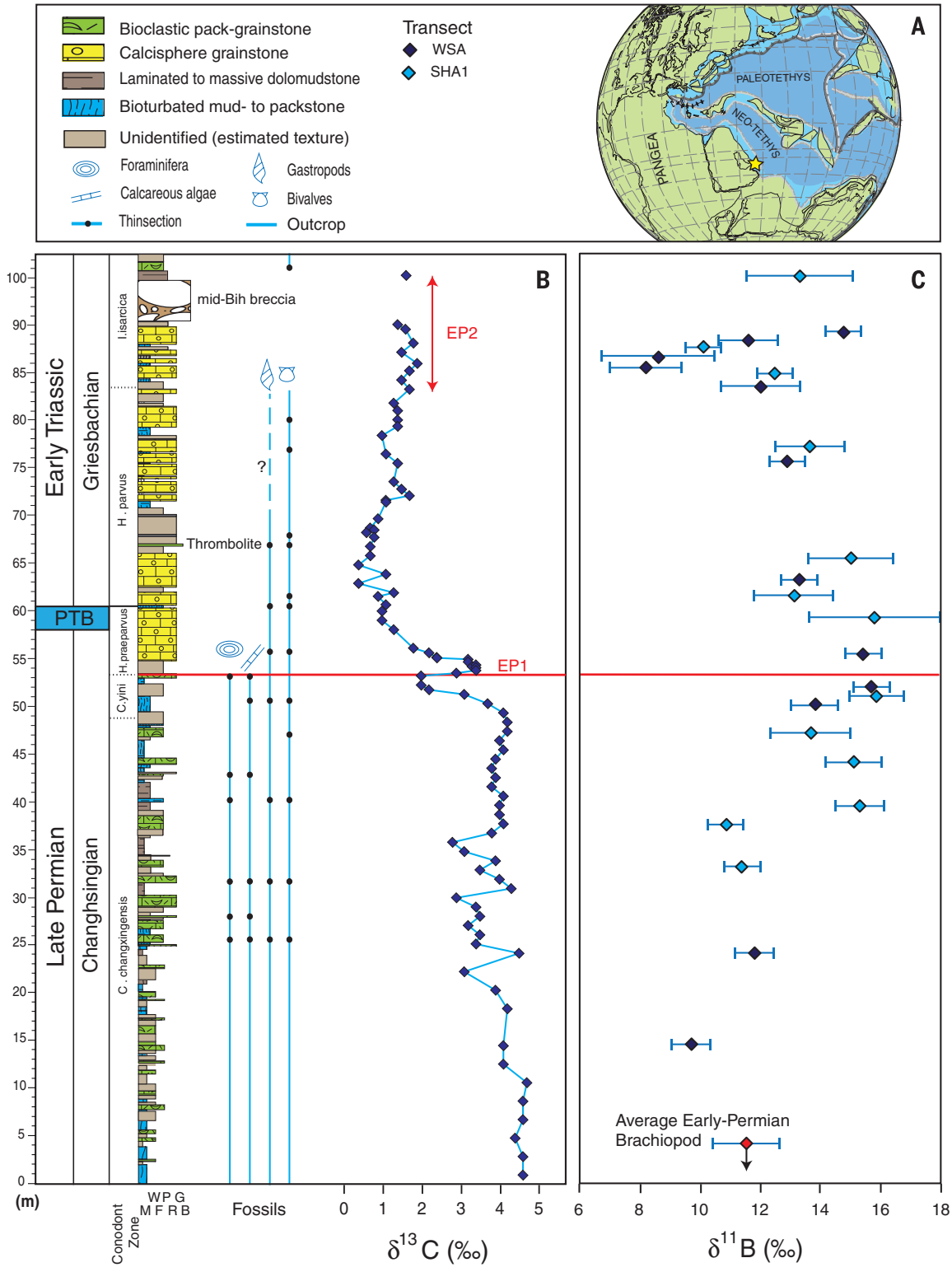

Fig. 1. Site locality and high-resolution carbon and boron isotope data. (**A**) Paleogeographic reconstruction for the Late Permian showing the studied section Wadi Bih, in the Musandam Mountains of U.A.E., that formed an extensive carbonate platform in the Neo-Tethyan Ocean. [Modified from (*35*).] (**B**) Shallow water $\delta^{13}C$ record (*18*). (**C**) Boron isotope ($\delta^{11}B$) record (propagated uncertainty given as $2\sigma_f$) and average Early Permian brachiopod value (n = 5 samples) (*19*). Lithology, biota, and transect key are provided in (A). Only *Hindeodus parvus* has been found so far in this section (*18*), and the conodont zones with dashed lines are identified from the $\delta^{13}C$ record and regional stratigraphy (*36*–*38*).

indicate only a minor temperature decrease of a few degrees celsius during the Changhsingian (*22*), suggesting that these mechanisms alone cannot explain the pH increase (fig. S5). Conversely, an increase in carbonate input or a reduction in rates of carbonate deposition both result in increases in Ω, with a greater impact on pH per unit decrease in P_{CO_2} and temperature (fig. S6).

A decrease in carbonate sedimentation is consistent with the decrease in depositional shelf area that occurred because of the second-order regression of the Late Permian (*23*). With the added expansion of anoxia into shelf environments (*24*), this would effectively create both bottom-up and top-down pressures to reduce the area of potential carbonate sedimentation.

Sea-level fall also exposed carbonates to weathering (*23*), which would have further augmented the alkalinity influx. The pH increase event supports the CO_2*Lo* initialization scenario [CO_2 ~3 present atmospheric levels (PAL), pH ~8, $\delta^{11}B_{SW}$ ~34‰] (supplementary text) because the simulated CO_2 and temperature decrease is much reduced and therefore is more consistent with

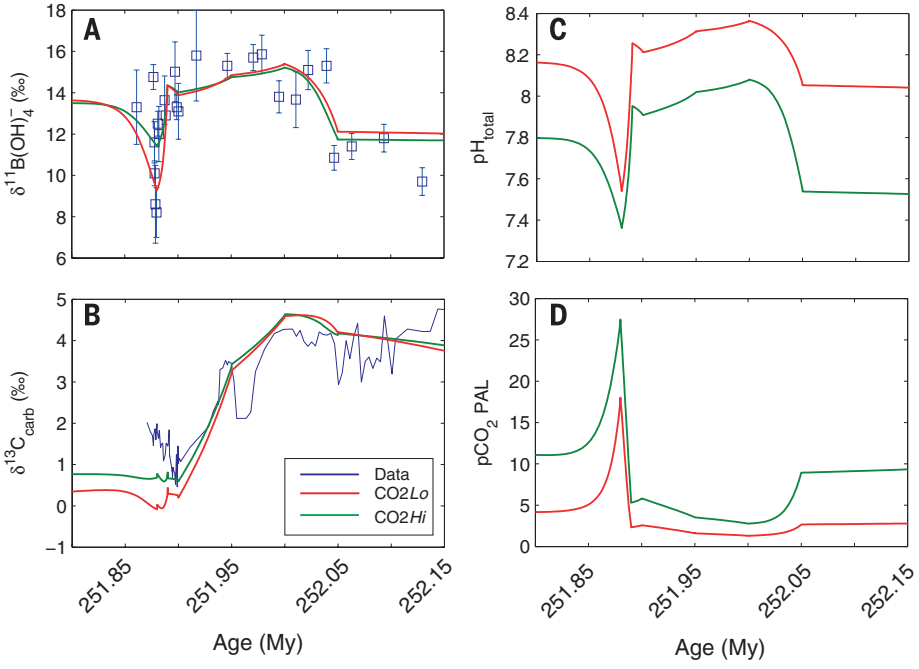

Fig. 2. Model results of carbon cycle parameters for high- and low-CO_2 end-member scenarios. (**A**) Model-reproduced $\delta^{11}B$ versus data. (**B**) Modeled $\delta^{13}C$ versus data. (**C**) Modeled pH envelope incorporating uncertainty of seawater B isotope composition ($\delta^{11}B_{SW}$) and dynamic temperatures. (**D**) Calculated atmospheric CO_2.

independent proxy data (*22*), as compared with CO_2*Hi* (CO_2 ~10 PAL, pH ~7.5, $\delta^{11}B_{SW}$ ~36.8‰) (Fig. 2D).

Before EP1, $\delta^{13}C_{carb}$ values began to decrease before reaching the minimum of the globally recognized negative CIE at the PTB (Fig. 1). At this time, both $\delta^{11}B$ and ocean pH remained stable. Hypotheses to explain the negative CIE require the input of isotopically light carbon, such as from volcanism (*14*, *25*), with the assimilation of very light organic carbon from the surrounding host rock (*26*), methane destabilization (*27*), collapse of the biological pump (*15*), and/or a decrease in the burial of terrestrial carbon (*16*). We can simulate the observed drop in $\delta^{13}C$, while remaining within the uncertainty of the $\delta^{11}B$ data (Fig. 2), by combining a cessation of terrestrial carbon burial with a relatively slow (50,000 years) carbon injection from any of the above sources (fig. S8). A small source of methane (3.2×10^{17} mol C with $\delta^{13}C = -50‰$) gives the least change in $\delta^{11}B$ and pH, whereas either a larger source of organic carbon (~6.5×10^{17} mol C with $\delta^{13}C = -25‰$) or a mixture of mantle and lighter carbon sources (~1.3×10^{18} mol C with $\delta^{13}C = -12.5‰$) are still within the measured uncertainty in $\delta^{11}B$.

This relatively slow addition of carbon minimizes the tendency for a transient decline in surface ocean pH in an ocean that was already primed with a high Ω and hence high buffering capacity from the Late Permian. The global presence of microbial and abiotic carbonate fabrics after EP1 (*28*) is indicative that this high Ω was maintained across the CIE. The carbon injection triggers an increase in P_{CO_2}, temperature, and silicate weathering, creating an additional counterbalancing alkalinity flux, which is consistent with independent proxy data (*6*). The alkalinity source may have been further increased through soil loss (*29*), the emplacement of easily weathered Siberian Trap basalt, or the impact of acid rain (*30*), which would have increased weathering efficiency.

The negative $\delta^{11}B_{carb}$ excursion at 251.88 Ma represents a calculated pH decrease of up to 0.7 pH. This pH decrease coincides with the second pulse of the extinction (Fig. 1), which preferentially affected the heavily calcifying, physiologically unbuffered, and sessile organisms (*3*). This was also accompanied by the temporary loss of abiotic and microbial carbonates throughout the Tethys (*31*, *32*), suggesting a coeval decrease in Ω. To overwhelm the buffering capacity of the ocean and decrease pH in this way requires a second, more abrupt injection of carbon into the atmosphere, yet remarkably, the acidification event occurs after the decline in $\delta^{13}C$, when $\delta^{13}C$ has rebounded somewhat and is essentially stable (Fig. 1).

Unlike the first carbon injection, the lack of change in $\delta^{13}C$ at this time rules out very ^{13}C-depleted carbon sources because no counterbalancing strongly ^{13}C-enriched source exists. Instead, it requires a carbon source near ~0‰. A plausible scenario for this is the decarbonation of overlying carbonate host rock, into which the Siberian Traps intruded (*26*), or the direct assimilation of carbonates and evaporites into the melt (*33*). Host carbonates would have had $\delta^{13}C$ ~ +2 to 4‰, which when mixed with mantle carbon (~−5‰) potentially produces a source near 0‰. We can simulate the sharp drop in pH and stable $\delta^{13}C$ values (Fig. 2) through a large and rapid carbon release of 2×10^{18} mol C over 10,000 years (fig. S8). This is undoubtedly a massive injection of 24,000 PgC at a rapid rate of 2.4 PgC/year, but it is physically plausible given existing estimates of the volume of carbonate host sediments subject to contact metamorphism and postulated mechanisms of carbon release (supplementary text). This second rapid carbon release produces a sharp rise in P_{CO_2} to ~20 PAL and warming of ~15°C, which is consistent with the observation of peak temperatures after EP1 (*22*). Initialization of the carbon cycle model under CO_2*Hi* cannot generate the magnitude of $\delta^{11}B$ drop (Fig. 2A) because the nonlinear relation between pH and $\delta^{11}B$ fractionation sets a lower limit of $\delta^{11}B$ at ~10‰ in this case (fig. S3). Thus, low initial CO_2 of ~3 PAL in the Late Permian (CO_2*Lo*) is more consistent with our data.

An acidification event of ~10,000 years is consistent with the modeled time scale required to replenish the ocean with alkalinity, as carbonate deposition is reduced and weathering is increased under higher P_{CO_2} and global temperatures. Increased silicate weathering rates drive further CO_2 drawdown, resulting in stabilization (Fig. 2D). High global temperature (*6*) and increased silicate weathering are consistent with a sudden increase in both $^{87}Sr/^{86}Sr$ (*34*) and sedimentation rates (*29*) in the Griesbachian.

The PTB was a time of extreme environmental change, and our combined data and modeling approach falsifies several of the mechanisms currently proposed. Although the coincident stresses of anoxia, increasing temperature, and ecosystem restructuring were important during this interval, the $\delta^{11}B$ record strongly suggests that widespread ocean acidification was not a factor in the first phase of the mass extinction but did drive the second pulse. The carbon release required to drive the observed acidification event must have occurred at a rate comparable with the current anthropogenic perturbation but exceeds it in expected magnitude. Specifically, the required model perturbation of 24,000 PgC exceeds the ~5000 PgC of conventional fossil fuels and is at the upper end of the range of estimates of unconventional fossil fuels (such as methane hydrates). We show that such a rapid and large release of carbon is critical to causing the combined synchronous decrease in both pH and saturation state that defines an ocean acidification event (*11*).

REFERENCES AND NOTES

1. D. H. Erwin, *Nature* **367**, 231–236 (1994).
2. S. D. Burgess, S. Bowring, S. Z. Shen, *Proc. Natl. Acad. Sci. U.S.A.* **111**, 3316–3321 (2014).
3. H. J. Song, P. B. Wignall, J. A. Tong, Y. Hongfu, *Nat. Geosci.* **6**, 52–56 (2012).
4. P. B. Wignall, R. J. Twitchett, *Science* **272**, 1155–1158 (1996).
5. K. Grice *et al.*, *Science* **307**, 706–709 (2005).
6. Y. Sun *et al.*, *Science* **338**, 366–370 (2012).
7. J. L. Payne *et al.*, *Proc. Natl. Acad. Sci. U.S.A.* **107**, 8543–8548 (2010).
8. A. H. Knoll, R. K. Barnbach, J. L. Payne, S. Pruss, W. W. Fischer, *Earth Planet. Sci. Lett.* **256**, 295–313 (2007).
9. J. L. Payne *et al.*, *Geol. Soc. Am. Bull.* **119**, 771–784 (2007).
10. C. Korte, H. W. Kozur, *J. Asian Earth Sci.* **39**, 215–235 (2010).

11. B. Hönisch *et al.*, *Science* **335**, 1058–1063 (2012).
12. C. L. Blättler, H. C. Jenkyns, L. M. Reynard, G. M. Henderson, *Earth Planet. Sci. Lett.* **309**, 77–88 (2011).
13. P. B. Wignall, S. Kershaw, P. Y. Collin, S. Crasquin-Soleau, *Geol. Soc. Am. Bull.* **121**, 954–956 (2009).
14. R. A. Berner, *Proc. Natl. Acad. Sci. U.S.A.* **99**, 4172–4177 (2002).
15. M. R. Rampino, K. Caldeira, *Terra Nova* **17**, 554–559 (2005).
16. W. S. Broecker, S. Peacock, *Global Biogeochem. Cycles* **13**, 1167–1172 (1999).
17. Materials and methods are available on *Science* Online
18. M. O. Clarkson *et al.*, *Gondwana Res.* **24**, 233–242 (2013).
19. M. M. Joachimski, L. Simon, R. van Geldern, C. Lecuyer, *Geochim. Cosmochim. Acta* **69**, 4035–4044 (2005).
20. The alternative way to drive an increase in pH would be through a removal of carbon; however, this would be evident in the $\delta^{13}C$ record, so we can rule it out.
21. Bacterial sulfate reduction (BSR) is a net source of alkalinity if the generated H_2S is buried as pyrite. Pyrite deposition is seen widely in certain settings during the Late Permian to PTB. Further information is provided in the supplementary materials.
22. M. M. Joachimski *et al.*, *Geology* **40**, 195–198 (2012).
23. H. Yin *et al.*, *Earth Sci. Rev.* **137**, 19–33 (2014).
24. P. B. Wignall, R. J. Twitchett, in *Catastrophic Events and Mass Extinctions: Impacts and Beyond*, C. Koeberl, K. G. MacLeod, Eds. (Geological Society of America, Boulder, CO, 2002), pp. 395–413.
25. C. Korte *et al.*, *J. Asian Earth Sci.* **37**, 293–311 (2010).
26. H. Svensen *et al.*, *Earth Planet. Sci. Lett.* **277**, 490–500 (2009).
27. E. S. Krull, G. J. Retallack, *Geol. Soc. Am. Bull.* **112**, 1459–1472 (2000).
28. A. D. Woods, *Earth Sci. Rev.* **137**, 6–18 (2013).
29. T. J. Algeo, Z. Q. Chen, M. L. Fraiser, R. J. Twitchett, *Palaeogeogr. Palaeoclimatol. Palaeoecol.* **308**, 1–11 (2011).
30. B. A. Black, J. F. Lamarque, C. A. Shields, L. T. Elkins-Tanton, J. T. Kiehl, *Geology* **42**, 67–70 (2014).
31. A. Baud, S. Richoz, S. Pruss, *Global Planet. Change* **55**, 81–89 (2007).
32. S. Richoz *et al.*, *J. Asian Earth Sci.* **39**, 236–253 (2010).
33. B. A. Black, L. T. Elkins-Tanton, M. C. Rowe, I. U. Peate, *Earth Planet. Sci. Lett.* **317**, 363–373 (2012).
34. C. Korte *et al.*, *Int. J. Earth Sci.* **93**, 565–581 (2004).
35. G. M. Stampfli, G. D. Borel, *Earth Planet. Sci. Lett.* **196**, 17–33 (2002).
36. S. Z. Shen *et al.*, *Earth Planet. Sci. Lett.* **375**, 156–165 (2013).
37. B. Koehrer *et al.*, *GeoArabia* **15**, 91–156 (2010).
38. F. Maurer, R. Martini, R. Rettori, H. Hillgartner, S. Cirilli, *GeoArabia* **14**, 125–158 (2009).

ACKNOWLEDGMENTS

M.O.C. acknowledges funding from the Edinburgh University Principal's Career Development Scholarship, the International Centre for Carbonate Reservoirs, and The Marsden Fund (U001314). R.A.W., T.M.L., and S.W.P. acknowledge support from the Natural Environment Research Council through the "Co-evolution of Life and the Planet" scheme (NE/I005978). T.M.L. and S.J.D. were supported by the Leverhulme Trust (RPG-2013-106). S.A.K. and A.M. acknowledge support from the German Research Foundation (Deutsche Forschungsgemeinschaft) Major Research Instrumentation Program INST 144/307-1. This is a contribution to IGCP 572, with S.R. sponsored for fieldwork by the Austrian National Committee (Austrian Academy of Sciences) for the International Geoscience Programme (IGCP). We are grateful to R. Newton and A. Thomas for helpful discussions, L. Krystyn for field assistance, F. Maurer for discussions on stratigraphy and providing photomicrographs, and B. Mills for assisting with model studies. Data are available online in the supplementary materials and at www.pangaea.de.

SUPPLEMENTARY MATERIALS

www.sciencemag.org/content/348/6231/229/suppl/DC1
Materials and Methods
Supplementary Text
Figs. S1 to S9
Tables S1 to S10
References (*39*–*98*)

8 October 2014; accepted 4 March 2015
10.1126/science.aaa0193

COMETARY FORMATION

Molecular nitrogen in comet 67P/Churyumov-Gerasimenko indicates a low formation temperature

M. Rubin,[1]* K. Altwegg,[1,2] H. Balsiger,[1] A. Bar-Nun,[3] J.-J. Berthelier,[4] A. Bieler,[1,5] P. Bochsler,[1] C. Briois,[6] U. Calmonte,[1] M. Combi,[5] J. De Keyser,[7] F. Dhooghe,[7] P. Eberhardt,[1]† B. Fiethe,[8] S. A. Fuselier,[9] S. Gasc,[1] T. I. Gombosi,[5] K. C. Hansen,[5] M. Hässig,[1,9] A. Jäckel,[1] E. Kopp,[1] A. Korth,[10] L. Le Roy,[2] U. Mall,[10] B. Marty,[11] O. Mousis,[12] T. Owen,[13] H. Rème,[14,15] T. Sémon,[1] C.-Y. Tzou,[1] J. H. Waite,[9] P. Wurz[1]

Molecular nitrogen (N_2) is thought to have been the most abundant form of nitrogen in the protosolar nebula. It is the main N-bearing molecule in the atmospheres of Pluto and Triton and probably the main nitrogen reservoir from which the giant planets formed. Yet in comets, often considered the most primitive bodies in the solar system, N_2 has not been detected. Here we report the direct in situ measurement of N_2 in the Jupiter family comet 67P/Churyumov-Gerasimenko, made by the Rosetta Orbiter Spectrometer for Ion and Neutral Analysis mass spectrometer aboard the Rosetta spacecraft. A N_2/CO ratio of $(5.70 \pm 0.66) \times 10^{-3}$ (2σ standard deviation of the sampled mean) corresponds to depletion by a factor of ~25.4 ± 8.9 as compared to the protosolar value. This depletion suggests that cometary grains formed at low-temperature conditions below ~30 kelvin.

Thermochemical models of the protosolar nebula (PSN) suggest that molecular nitrogen (N_2) was the principal nitrogen species during the disk phase (*1*) and that the nitrogen present in the giant planets was accreted in this form (*2*). Moreover, Pluto and Triton, which are both expected to have formed in the same region of the PSN as Jupiter family comets (JFCs), have N_2-dominated atmospheres and surface deposits of N_2 ice (*3*, *4*). This molecule has never been firmly detected in comets; however, CN, HCN, NH, NH_2, and NH_3 among others have been observed spectroscopically (*5*, *6*). The abundance of N_2 in comets is therefore a key to understanding the conditions in which they formed.

Condensation or trapping of N_2 in ice occurs at similar thermodynamic conditions as those needed for CO in the PSN (*7*, *8*). This requires very low PSN temperatures and implies that the detection of N_2 in comets and its abundance ratio with respect to CO would put strong constraints on comet formation conditions (*7*, *8*). Ground-based spectroscopic observations of the N_2^+ band in the near ultraviolet are very difficult because of the presence of telluric N_2^+ and other cometary emission lines. Searches conducted with high-resolution spectra of comets 122P/de Vico, C/1995 O1 (Hale-Bopp), and 153P/2002 C1 (Ikeya-Zhang) have been unsuccessful and yielded upper limits of 10^{-5} to 10^{-4} for the N_2^+/CO^+ ratio (*9*, *10*). Only one N_2^+ detection in C/2002 VQ94 (LINEAR) from ground-based observations is convincing, because the comet was at sufficient distance from the Sun to prevent terrestrial twilight N_2^+ contamination (*11*). The in situ measurements made by Giotto in 1P/Halley were inconclusive, because the resolution of the mass spectrometers aboard the spacecraft (*12*) was insufficient to separate the nearly identical masses of N_2 and CO during the 1P/Halley encounter, and only an upper limit could be derived for the relative production rates $[Q(N_2)/Q(CO) \leq 0.1]$ (*13*).

Here we report the direct in situ measurement of the N_2/CO ratio by the Rosetta Orbiter Spectrometer for Ion and Neutral Analysis (ROSINA)

[1]Physikalisches Institut, University of Bern, Sidlerstrasse 5, CH-3012 Bern, Switzerland. [2]Center for Space and Habitability, University of Bern, Sidlerstrasse. 5, CH-3012 Bern, Switzerland. [3]Department of Geoscience, Tel-Aviv University, Ramat-Aviv, Tel-Aviv, Israel. [4]Laboratoire Atmosphères, Milieux, Observations Spatiales (LATMOS)/Institute Pierre Simon Laplace–CNRS-UPMC-UVSQ, 4 Avenue de Neptune F-94100, Saint-Maur, France. [5]Department of Atmospheric, Oceanic and Space Sciences, University of Michigan, 2455 Hayward, Ann Arbor, MI 48109, USA. [6]Laboratoire de Physique et Chimie de l'Environnement et de l'Espace (LPC2E), UMR 6115 CNRS–Université d'Orléans, Orléans, France. [7]Belgian Institute for Space Aeronomy, Belgisch Instituut voor Ruimte-Aeronomie–Institut d'Aéronomie Spatiale de Belgique (BIRA-IASB), Ringlaan 3, B-1180 Brussels, Belgium. [8]Institute of Computer and Network Engineering, Technische Universität Braunschweig, Hans-Sommer-Straße 66, D-38106 Braunschweig, Germany. [9]Department of Space Science, Southwest Research Institute, 6220 Culebra Road, San Antonio, TX 78228, USA. [10]Max-Planck-Institut für Sonnensystemforschung, Justus-von-Liebig-Weg 3, 37077 Göttingen, Germany. [11]Centre de Recherches Pétrographiques et Géochimiques (CRPG)–CNRS, Université de Lorraine, 15 rue Notre Dame des Pauvres, Bôite Postale 20, 54501 Vandoeuvre lès Nancy, France. [12]Aix Marseille Université, CNRS, Laboratoire d'Astrophysique de Marseille UMR 7326, 13388, Marseille, France. [13]Institute for Astronomy, University of Hawaii, Honolulu, HI 96822, USA. [14]Université de Toulouse; UPS-OMP; Institut de Recherche en Astrophysique et Planétologie (IRAP), Toulouse, France. [15]CNRS; IRAP; 9 Avenue du Colonel Roche, Boîte Postale 44346, F-31028 Toulouse Cedex 4, France.
*Corresponding author. E-mail: martin.rubin@space.unibe.ch
†Deceased.

Ocean acidification and the Permo-Triassic mass extinction

M. O. Clarkson *et al.*

Science **348**, 229 (2015);
DOI: 10.1126/science.aaa0193

Science (print ISSN 0036-8075; online ISSN 1095-9203) is published weekly, except the last week in December, by the American Association for the Advancement of Science, 1200 New York Avenue NW, Washington, DC 20005.